Light-Induced-Magnetoresistance in *p-n* Junction Device

Yang Cao, Wenbo Sui, Tao Wang, Mingsu Si, Huigang Shi, Dezheng Yang, and Desheng Xue

***Abstract*—It is highly desirable to provide extra functionality for *p-n* junction to bypass the limits to Moore's law. By combining magnetoelectric and photovoltaic effects of *p-n* junctions, we demonstrate a novel light-induced magnetoresistance (MR) effect, that the photovoltage in the conventional *p-n* junction can be significantly tuned by magnetic field. In contrast to the symmetric MR driven by external electric field, light-induced MR presents an asymmetric behavior at positive and negative magnetic induction. Theoretical fits using photovoltaic transport equations further reveal that the asymmetric MR induced by light directly reflects the asymmetric geometric of the space-charge region in *p-n* junction under the magnetic induction. The results not only further confirm our MR model of *p-n* junction, but also provide a new route by using magnetic control of energy flow in light harvest.**

***Index Terms*—*p-n* junction, magnetoresistance, magnetoelectric effect, photovoltaic effect, space charge region.**

I. Introduction

WITH the extreme scaling of the semiconductor devices to pursue the predication of the Moore's law [1], *p-n* junctions, as the elementary building blocks in modern electronics, will soon reach their physical limitations. Since the discovery of the large magnetoresistance (MR) effect in semiconductor materials themselves, i.e. Si [2]–[8], Ge [9]–[11] and GaAs [12], [13], etc., it has become natural and necessary to integrate the magnetic functionalities into *p-n* junctions as an alternative methodology to bypass the Moore's law [14]–[16].

By modulating the space charge region (SCR) under the magnetic field without changing the CMOS-based technology, a significant magnetoelectric effect in conventional *p-n* junction has been observed [17]–[21]. This makes the *p-n* junction not only work as a basic electrical building block in modern electronics, but also function as the magnetic rectifier [15], [22]–[24], the magnetic amplifier [20], [25] and the magnetic logic operations [26], [27].

On the other side, *p-n* junction also has a significant photovoltaic effect, which plays an important role in conversion of energy of light harvest, i.e. photodetector and solar cells. During the illumination of light, the built-in electric field of SCR of *p-n* junction can effectively separate the photogenerated electron-hole pairs, and drive the electrons and holes move to the opposite regions to form the photovoltage (V_p). Because V_p also depends on the SCR of *p-n* junction according to the above scenario, this indicates that photovoltaic effect in the conventional *p-n* junction is also possible to be changed by modulating SCR under the magnetic induction, which will directly combine magnetoelectric and photovoltaic effects of *p-n* junction together [28], [29].

In this work, we investigate the MR effect of *p-n* junction illuminated by light. Compared with symmetric MR of *p-n* junction without illumination, the MR of *p-n* junction with illumination presents an obvious asymmetry with respect to external magnetic induction ($\boldsymbol{B}$), namely MR($\boldsymbol{B}$) $\neq$ MR($-\boldsymbol{B}$). With further decreasing the measurement current to the photocurrent region to avoid the affection of external electric field, the light-induced asymmetric MR can be well described by the photovoltaic transport equations, where current is considered to have a deflection due to the asymmetric geometry of the space-charge region in *p-n* junction under the magnetic induction.

II. Results and Discussion

Figure 1(a) shows schematic diagram of *p-n* junction device structure and measurement configuration. The *p-n* junction device was fabricated by ion implantation. The implantation concentration of Si($p+$) and Si($n+$) were 2.0×10^{14} cm^{-3} and 10^{15} cm^{-3}, respectively. During the measurement, a laser beam was used to irradiate on the side of $p+$ region, as shown in Fig. 1(a). The wavelength of the laser is 650 nm and the power of the laser is 30 mW. In order to generate a maximum Lorentz force, $\boldsymbol{B}$ was perpendicular to the current. During the measurements, we use Keithley 6221 as current source and Keithley 2182 as voltmeter.

Figure 1(b) shows the $\boldsymbol{B}$-modified *I-V* characteristics of the *p-n* junction with and without laser illumination at $T = 10$ K. All the *I-V* curves exhibit rectifying effects, indicating that the SCR plays a dominant role for the *p-n* junction transport. When laser is on, the *p-n* junction device presents a significant photovoltaic effect. The open-circuit photovoltage $V_{OC} = 1.1$ V, and the short-circuit photocurrent $I_{SC} = 50.0$ μA. Interestingly, for the two situations with and without illumination, the $\boldsymbol{B}$-modulated *I-V* characteristics of *p-n* junction device are completely different. For the *p-n* junction device without illumination, the *I-V* curves are shifted toward positive voltage region under the magnetic induction. For $\boldsymbol{B} = \pm 200$ mT the $\boldsymbol{B}$-modulated *I-V* characteristics almost coincide, indicating a symmetric MR effect. While, for the *p-n* junction device with illumination,

Manuscript received January 16, 2020; accepted January 23, 2020. Date of publication January 28, 2020; date of current version February 25, 2020. This work was supported in part by the NSFC of China under Grant 11774139, Grant 11874189, and Grant 11674143, in part by the Program for Changjiang Scholars and Innovative Research Team (PCSIRT) under Grant IRT-16R35, and in part by the Program for Science and Technology of Gansu Province under Grant 17YF1GA024. The review of this letter was arranged by Editor B. G. Malm. *(Corresponding authors: Dezheng Yang; Desheng Xue.)*

The authors are with the Key Laboratory for Magnetism and Magnetic Materials of the Ministry of Education, Lanzhou University, Lanzhou 730000, China (e-mail: yangdzh@lzu.edu.cn; xueds@lzu.edu.cn).

Color versions of one or more of the figures in this letter are available online at http://ieeexplore.ieee.org.

Digital Object Identifier 10.1109/LED.2020.2969998

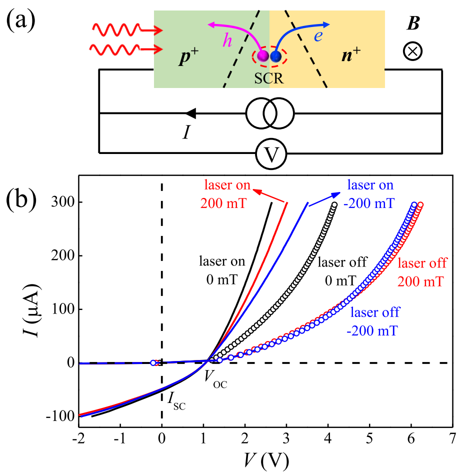

Fig. 1. (a) Schematic diagram of *p-n* junction device structure and measurement configuration. (b) The ***B***-modulated *I-V* characteristics of the *p-n* junction device with and without illumination.

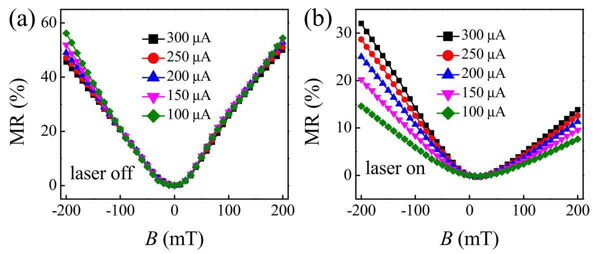

Fig. 2. MR without (a) and with illumination (b) at various currents. MR curves with (without) illumination is asymmetric (symmetric) with respect to ***B***.

the *I-V* are also shifted toward positive voltage region under the magnetic induction, but for $\boldsymbol{B} = \pm$ 200 mT the ***B***-modulated *I-V* characteristics are separated, indicating an asymmetric MR effect. It should be noted that the symmetric MR effects driven by external electric field are consistent with the previous reports [17]–[21], but to our knowledge, the asymmetric MR effect of *p-n* junction driven by light have not been reported yet. Moreover, the amplitude of voltage variations induced by magnetic induction is extremely large (∼ V), thus we can exclude the heat-induced MR, where the amplitude of thermal signal is extremely small (∼ μV).

To clearly demonstrate the asymmetry of the MR effect of *p-n* junction driven by light, we measured the MR curves without and with illumination at various external electrical currents. Here, MR is defined as MR(%)=$[V(\boldsymbol{B})-V(0)]/V(0)$, where $V(\boldsymbol{B})$ and $V(0)$ are the voltage of *p-n* junction device with and without ***B***, respectively. Figure 2(a) shows the MR curves of the *p-n* junction device without illumination. The MR curves are symmetric and approximately quadratic for all currents. This indicates that the electric-field-induced MR effect is symmetric with ***B***. However, for the *p-n* junction device with illumination in Fig. 2(b), the MR curves are asymmetric with ***B***. The MR ratio at negative ***B*** is larger than the MR ratio at positive ***B***. With further increasing the electric current, the asymmetry of MR gradually increases. This indicates that the observed asymmetric MR stems from both the light-induced MR and electric-field-induced MR. Compared with the symmetric electric-field-induced MR effect in Fig. 2(a), one can conclude that the asymmetric component of MR should origin from the light-induced MR effect.

In order to further eliminate the electric-field-induced MR effect, we measured the MR curves close to V_{OC} region, where the external electric current is almost negligible. As can be seen from Fig. 3(a), the MR curves close to V_{OC} region are all asymmetric with ***B***, but present different MR behaviors. At positive current regions MR curves open upward, while at negative current regions MR curves open downward. In particular, for $I = 0$ μA it should be noted that the electric-field-induced MR effect is completely eliminated. At this point, one can find that the MR curve is almost completely anti-symmetric. Moreover, the MR curve at $I = 0$ μA also demonstrates that the open-circuit photovoltage V_{OC} can be modulated by ***B***, which will be useful for potential magnetic control of photoelectric conversion efficiency in conventional *p-n* junctions.

In order to quantitatively describe the light-induced MR effect, we analyze photovoltaic transport equations under the external magnetic induction. For simplify, we considered the situation that the carrier is electron. For carrier is hole, the discussion is similar.

$$\frac{\partial n}{\partial t} = \frac{1}{q}\nabla \cdot \boldsymbol{J}_n + G(x) - U = 0, \tag{1}$$

where q is the carrier charge, t is the time, n is the electron concentrations, $\boldsymbol{J}_n$ is photocurrent densities for electrons, x is the distance far from the light source, $G(x)$ represents the carrier generation rate induced by light, which is exponential decay with x, and U represents the carrier recombination rate. Equation (1) represents the continuity equations of electron. The variation of carrier concentrations in this region depends on current flowing in/out (first term), the light-generated carriers (second term) and the carrier recombination (the third term). For the stable condition, $\frac{\partial n}{\partial t} = 0$.

Here $\boldsymbol{J}_n$ under the magnetic induction ***B*** is described by the following equation, which includes the drift current (first term), the diffusion current (second term) and the Lorentz force induced current (the third term), [21]

$$\boldsymbol{J}_n = q\mu_n n\boldsymbol{E} + qD_n\nabla n - q\mu_n n\boldsymbol{v}_n \times \boldsymbol{B}, \tag{2}$$

where μ_{n} is the electron mobility, D_{n} is the electron diffusivity, ***E*** is the electric field and $\boldsymbol{v}_n$ is the electron drift velocity. In order to get the analytical solution, we make an approximation,

$$\boldsymbol{J}_n = nq\boldsymbol{v}_n. \tag{3}$$

Strictly speaking, the velocity $\boldsymbol{v}_n$ is not proportional to the total current density $\boldsymbol{J}_n$, since $\boldsymbol{J}_n$ is the sum of drift and diffusion currents. However, under the condition of the drift current much larger than the diffusion current, the approximation of Eq. (3) is valid and has been used for other models in literature [30]–[32]. For our model, the photocurrent of the *p-n* junction originates from the fact that photogenerated electron-hole pairs are separated by the strong electric field of SCR. In this situation, the drift current is much larger than the diffusion current [33], indicating the approximation is also reasonable.

In order to get analytical solution of $\boldsymbol{J}_n(\boldsymbol{B})$ for Eqs. (1), (2) and (3), we consider the Lorentz force induced current in Eq. (2) as a perturbation item. For $\boldsymbol{B} = 0$, we define $\boldsymbol{J}_n(0)$ is the exact solution of Eqs. (1), (2) and (3). When ***B*** is applied, Eqs. (2) and (3) could be rewritten by replacing $\boldsymbol{J}_n$ on the item of Lorentz force induced current,

$$\boldsymbol{J}_n = q\mu_n n\boldsymbol{E} + qD_n\nabla n - \mu_n(q\mu_n n\boldsymbol{E} + qD_n\nabla n - \mu_n\boldsymbol{J}_n \times \boldsymbol{B}) \times \boldsymbol{B}. \tag{4}$$

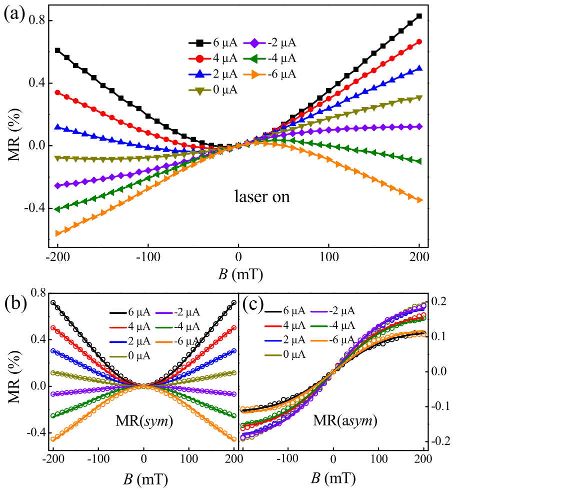

Fig. 3. (a) The MR curves with illumination close to V_{OC} region. (b) and (c) are the symmetric components and anti-symmetric components extracted from the MR curves with illumination, respectively. The hollow circles are the data points. The solid lines are the corresponding fit with Eq. (6).

By utilizing $(\boldsymbol{J}_n \times \boldsymbol{B}) \times \boldsymbol{B} = (\boldsymbol{B} \cdot \boldsymbol{J}_n)\, \boldsymbol{B} - B^2 \boldsymbol{J}_n = -B^2 \boldsymbol{J}_n$ (for $\boldsymbol{B} \perp \boldsymbol{J}_n$), we can obtain the solution of photocurrent under the magnetic induction $\boldsymbol{J}_n(\boldsymbol{B})$,

$$\boldsymbol{J}_n(\boldsymbol{B}) = \frac{1}{1+\mu_n^2 B^2}\left(\boldsymbol{J}_n(0) - \mu_n \boldsymbol{J}_n(0) \times \boldsymbol{B}\right). \qquad (5)$$

Remarkably, the second term $-\mu_n \boldsymbol{J}_n(0) \times \boldsymbol{B}$ represents the current deflection caused by the Lorentz force. For a uniform semiconductor, this term is usually compensated by Hall field, due to the carrier charge accumulation at the boundary. Interestingly, the second term can exist in *p-n* junction. This is because there are not enough mobilizable carriers in SCR to compensate the Lorentz force. Instead, a trapezoidal distribution of SCR in Fig. 1(a) is formed, which induces carrier concentration deviation to balance the Lorentz force [21]. This estimate is also confirmed by experiments [17]–[20]. Because of $\nabla \cdot (\boldsymbol{J}_n(0) \times \boldsymbol{B}) = 0$, $\boldsymbol{J}_n(\boldsymbol{B})$ in the Eq. (5) can be considered as the approximation solution of the Eq. (1). Because $G(x)$ and U are both associated with the geometry of SCR, the trapezoidal distribution of SCR under magnetic induction will further amplify the deflection of current. Therefore, MR effect of *p-n* junction with illumination should be proportional to $\Delta \boldsymbol{J}_n = \boldsymbol{J}_n(\boldsymbol{B}) - \boldsymbol{J}_n(0)$, thus

$$\mathrm{MR}(B) = C_{sym}\left(1 - \frac{1}{1+\mu_n^2 B^2}\right) + C_{asym}\frac{\mu_n B}{1+\mu_n^2 B^2}, \qquad (6)$$

where C_{sym} and C_{asym} are the coefficients of symmetric and anti-symmetric components of MR with illumination, respectively. Obviously, the symmetric component of MR (even function) stems from the electric-field-induced MR, while the anti-symmetric component of MR (odd function) stems from the light-induced MR, which represents the current deflection caused by the Lorentz force.

The symmetric and anti-symmetric components of MR curves with illumination can be simply decomposed by the following mathematical processing,

$$\mathrm{MR}\,(sym) = \frac{1}{2}(\mathrm{MR}\,(\boldsymbol{B}) + \mathrm{MR}\,(-\boldsymbol{B})), \qquad (7.1)$$

$$\mathrm{MR}\,(asym) = \frac{1}{2}(\mathrm{MR}\,(\boldsymbol{B}) - \mathrm{MR}\,(-\boldsymbol{B})), \qquad (7.2)$$

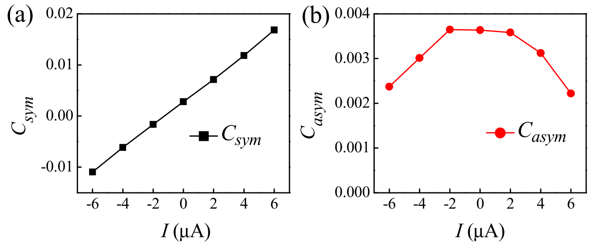

Fig. 4. The coefficients C_{sym} (a) and C_{asym} (b) for symmetric and anti-symmetric components of MR with illumination as functions of I, respectively.

which are shown in Fig. 3(b) and Fig. 3(c), respectively. We fitted all the MR data with various current well with Eq. (6). During the fitting, the mobility $\mu = 4.3 \times 10^4$ cm^{2}s^{-1}V^{-1} is consistent with the experimental values.

The two corresponding fitting parameters C_{sym} and C_{asym} are obtained and shown in Fig. 4(a) and (b), respectively. C_{sym} is proportional to the current, indicating that the width of SCR is modulated by the current. According to Fig. 3(c) and Fig. 4(b), C_{asym} is slightly decreased with the increasing absolute value of current, while Fig. 2(b) demonstrates a reverse trend, where the asymmetry of MR gradually increases with increasing the current. This is because the MR of *p-n* junction not only depends on the deflection of SCR caused by magnetic field, but also depends on the width of SCR caused by electric field. According to our previous experiments [17], [18] and theories [21], MR effect is obviously improved with increasing the applied current, demonstrating that the MR ratio is more sensitive to $\boldsymbol{B}$ in the narrower SCR. Thus, the reverse trend in Fig. 2(b) can be attributed to electric field effect, where the light amplification effect becomes more significant at the larger current region. In Fig. 3(c) and Fig. 4(b) electric-field-induced MR effect can be excluded, since we measured the MR curves close to zero current region. Thus, the fact that C_{asym} is slightly decreased with the increasing absolute value of current origins from the light-induced MR effect. Remarkably, the broken symmetry $\mathrm{MR}(\boldsymbol{B}) \neq \mathrm{MR}(-\boldsymbol{B})$ usually indicates the violation of the time reversal invariance [34], [35]. We ascribe the origin of light-induced asymmetry MR effect to the current deflection, which causes an additional Hall voltage breaking the time reversal.

III. Conclusion

In conclusion, we reported a light-induced MR of *p-n* junction, which can naturally integrate magnetoelectronic effect and photoelectronic effect together. Unlike conventional symmetric MR induced by electric field, the light-induced MR of *p-n* junction presents an asymmetric behavior. The newly discovered effect can be satisfactorily explained by light-induced amplification effect due to asymmetric geometry SCR under magnetic induction. The results in this work report a fact that the photovoltage of conventional *p-n* junction can be modified by magnetic induction. These results might provide a new idea by the magnetic control of energy flow in light harvest, and indicate that the conventional *p-n* junction can be used as a multifunctional material based on the interplay between electronic, magnetic and optic response together, which is significant for future semiconductor industry.

References

[1] M. M. Waldrop, "The semiconductor industry will soon abandon its pursuit of Moore's law. Now things could get a lot more interesting," *Nature*, vol. 530, no. 7589, pp. 144–147, Feb. 2016, doi: 10.1038/530144a.

[2] J. J. H. M. Schoonus, F. L. Bloom, W. Wagemans, H. J. M. Swagten, and B. Koopmans, "Extremely large magnetoresistance in boron-doped silicon," *Phys. Rev. Lett.*, vol. 100, no. 12, Mar. 2008, Art. no. 127202, doi: 10.1103/PhysRevLett.100.127202.

[3] M. P. Delmo, S. Yamamoto, S. Kasai, T. Ono, and K. Kobayashi, "Large positive magnetoresistive effect in silicon induced by the space-charge effect," *Nature*, vol. 457, no. 7233, pp. 1112–1115, Feb. 2009, doi: 10.1038/nature07711.

[4] M. P. Delmo, S. Kasai, K. Kobayashi, and T. Ono, "Current-controlled magnetoresistance in silicon in non-ohmic transport regimes," *Appl. Phys. Lett.*, vol. 95, no. 13, Sep. 2009, Art. no. 132106, doi: 10.1063/1.3238361.

[5] C. Wan, X. Zhang, X. Gao, J. Wang, and X. Tan, "Geometrical enhancement of low-field magnetoresistance in silicon," *Nature*, vol. 477, no. 7364, pp. 304–307, Sep. 2011, doi: 10.1038/nature10375.

[6] R. Singh, Z. Luo, Z. Lu, A. S. Saleemi, C. Xiong, and X. Zhang, "Diode and inhomogeneity assisted extremely large magnetoresistance in silicon," *Appl. Phys. Lett.*, vol. 111, no. 4, Jul. 2017, Art. no. 042406, doi: 10.1063/1.4996493.

[7] Z. Luo, H.-G. Piao, A. V. Brooks, X. Wang, J. Chen, C. Xiong, F. Yang, X. Wang, X.-G. Zhang, and X. Zhang, "Large magnetoresistance in silicon at room temperature induced by onsite Coulomb interaction," *Adv. Electron. Mater.*, vol. 3, no. 9, Sep. 2017, Art. no. 1700186, doi: 10.1002/aelm.201700186.

[8] Y. Zhang, J. Fan, Q. Huang, J. Zhu, Y. Zhao, M. Li, Y. Wu, and R. Huang, "Voltage-controlled magnetoresistance in silicon nanowire transistors," *Sci. Rep.*, vol. 8, no. 1, Dec. 2018, Art. no. 15194, doi: 10.1038/s41598-018-33673-8.

[9] K. Zhang, H. Li, P. Grunberg, Q. Li, S. Ye, Y. Tian, S. Yan, Z. Lin, S. Kang, Y. Chen, G. Liu, and L. Mei, "Large rectification magnetoresistance in nonmagnetic Al/Ge/Al heterojunctions," *Sci. Rep.*, vol. 5, no. 1, p. 14249, Nov. 2015, doi: 10.1038/srep14249.

[10] J. Chen, H.-G. Piao, Z. Luo, and X. Zhang, "Enhanced linear magnetoresistance of germanium at room temperature due to surface imperfection," *Appl. Phys. Lett.*, vol. 106, no. 17, Apr. 2015, Art. no. 173503, doi: 10.1063/1.4919216.

[11] B. Cheng, H. Qin, and J. Hu, "The measured positive and negative magnetoresistance for n-type germanium at room temperature," *J. Phys. D, Appl. Phys.*, vol. 50, no. 44, Nov. 2017, Art. no. 445001, doi: 10.1088/1361-6463/aa8b97.

[12] Z. G. Sun, M. Mizuguchi, T. Manago, and H. Akinaga, "Magnetic-field-controllable avalanche breakdown and giant magnetoresistive effects in Gold/semi-insulating-GaAs Schottky diode," *Appl. Phys. Lett.*, vol. 85, no. 23, pp. 5643–5645, Dec. 2004, doi: 10.1063/1.1834733.

[13] J. Xu, M. Ma, M. Sultanov, Z. Xiao, Y. Wang, D. Jin, Y. Lyu, W. Zhang, L. N. Pfeiffer, K. W. West, K. W. Baldwin, M. Shayegan, and W. K. Kwok, "Negative longitudinal magnetoresistance in gallium arsenide quantum wells," *Nature Commun.*, vol. 10, no. 1, p. 287, Dec. 2019, doi: 10.1038/s41467-018-08199-2.

[14] Q. Huang, Y. Yan, K. Zhang, H. Li, S. Kang, and Y. Tian, "Room temperature electrically tunable rectification magnetoresistance in Ge-based Schottky devices," *Sci. Rep.*, vol. 6, no. 1, Dec. 2016, Art. no. 37748, doi: 10.1038/srep37748.

[15] Q. Huang, J. Wang, S. Lu, Y. Chen, L. Bai, Y. Dai, Y. Tian, and S. Yan, "Distinguishing interface magnetoresistance and bulk magnetoresistance through rectification of Schottky heterojunctions," *ACS Appl. Mater. Interfaces*, vol. 10, no. 29, pp. 24905–24909, Jul. 2018, doi: 10.1021/acsami.8b06929.

[16] X. He, B. He, H. Yu, Z. Sun, J. He, and W. Zhao, "Separating interface magnetoresistance from bulk magnetoresistance in silicon-based Schottky heterojunctions device," *J. Appl. Phys.*, vol. 125, no. 22, Jun. 2019, Art. no. 224502, doi: 10.1063/1.5097736.

[17] D. Yang, F. Wang, Y. Ren, Y. Zuo, Y. Peng, S. Zhou, and D. Xue, "A large magnetoresistance effect in p–n junction devices by the space-charge effect," *Adv. Funct. Mater.*, vol. 23, no. 23, pp. 2918–2923, Jun. 2013, doi: 10.1002/adfm.201202695.

[18] T. Wang, M. Si, D. Yang, Z. Shi, F. Wang, Z. Yang, S. Zhou, and D. Xue, "Angular dependence of the magnetoresistance effect in a silicon based p–n junction device," *Nanoscale*, vol. 6, no. 8, pp. 3978–3983, Jan. 2014, doi: 10.1039/c3nr04077a.

[19] D. Yang, T. Wang, W. Sui, M. Si, D. Guo, Z. Shi, F. Wang, and D. Xue, "Temperature-dependent asymmetry of anisotropic magnetoresistance in silicon p–n junctions," *Sci. Rep.*, vol. 5, no. 1, Sep. 2015, Art. no. 11096, doi: 10.1038/srep11096.

[20] T. Wang, D. Yang, M. Si, F. Wang, S. Zhou, and D. Xue, "Magnetoresistance amplification effect in silicon transistor device," *Adv. Electron. Mater.*, vol. 2, no. 9, Sep. 2016, Art. no. 1600174, doi: 10.1002/aelm.201600174.

[21] Y. Cao, D. Yang, M. Si, H. Shi, and D. Xue, "Model for large magnetoresistance effect in p–n junctions," *Appl. Phys. Express*, vol. 11, no. 6, 2018, Art. no. 061304, doi: 10.7567/APEX.11.061304.

[22] K. Zhang, Q. Huang, Y. Yan, X. Wang, J. Wang, S. Kang, and Y. Tian, "Rectification magnetoresistance device: Experimental realization and theoretical simulation," *Appl. Phys. Lett.*, vol. 109, no. 21, Nov. 2016, Art. no. 213503, doi: 10.1063/1.4968784.

[23] X. Liu and W. Mi, "Electronic transport properties and magnetoresistance in the Fe_3O_4/SiO_2/p-Si heterostructure with an in-plane current geometry," *Phys. Chem. Chem. Phys.*, vol. 21, no. 14, pp. 7518–7523, Mar. 2019, doi: 10.1039/c9cp00033j.

[24] X. Liu, W. Mi, Q. Zhang, and X. Zhang, "Negative differential resistance and magnetotransport in $Fe_3O_4/SiO_2/Si$ heterostructures," *Appl. Phys. Lett.*, vol. 114, no. 24, Jun. 2019, Art. no. 242402, doi: 10.1063/1.5092872.

[25] H. Kum, S. Jahangir, D. Basu, D. Saha, and P. Bhattacharya, "Gate control and amplification of magnetoresistance in a three-terminal device," *Appl. Phys. Lett.*, vol. 99, no. 15, Oct. 2011, Art. no. 152503, doi: 10.1063/1.3652765.

[26] Z. Luo, X. Zhang, C. Xiong, and J. Chen, "Silicon-based current-controlled reconfigurable magnetoresistance logic combined with non-volatile memory," *Adv. Funct. Mater.*, vol. 25, no. 1, pp. 158–166, Jan. 2015, doi: 10.1002/adfm.201402955.

[27] K. Zhang, Y. Zhang, Z. Zhang, Z. Zheng, G. Wang, Y. Zhang, Q. Liu, S. Yan, and W. Zhao, "Large magnetoresistance and Boolean logic functions based on a ZnCoO film and diode combined device," *Adv. Electron. Mater.*, vol. 5, no. 3, Mar. 2019, Art. no. 1800812, doi: 10.1002/aelm.201800812.

[28] S. Wang, W. Wang, L. Zou, X. Zhang, J. Cai, Z. Sun, B. Shen, and J. Sun, "Magnetic tuning of the photovoltaic effect in silicon-based Schottky junctions," *Adv. Mater.*, vol. 26, no. 47, pp. 8059–8064, Dec. 2014, doi: 10.1002/adma.201403868.

[29] T.-Y. Lin, K.-T. Lin, C.-C. Lin, Y.-W. Lee, L.-T. Shiu, W.-Y. Chen, and H.-L. Chen, "Magnetic fields affect hot electrons in silicon-based photodetectors at telecommunication wavelengths," *Mater. Horizons*, vol. 6, no. 6, pp. 1156–1168, May 2019, doi: 10.1039/c9mh00295b.

[30] W. Allegretto, A. Nathan, and H. Baltes, "Numerical analysis of magnetic-field-sensitive bipolar devices," *IEEE Trans. Comput.-Aided Des. Integr. Circuits Syst.*, vol. 10, no. 4, pp. 501–511, Apr. 1991, doi: 10.1109/43.75633.

[31] L. Andor, H. Baltes, A. Nathan, and H. Schmidt-Weinmar, "Numerical modeling of magnetic-field-sensitive semiconductor devices," *IEEE Trans. Electron Devices*, vol. ED-32, no. 7, pp. 1224–1230, Jul. 1985, doi: 10.1109/t-ed.1985.22105.

[32] H. Pfleiderer, "Magnetodiode model," *Solid-State Electron.*, vol. 15, no. 3, pp. 335–353, Mar. 1972, doi: 10.1016/0038-1101(72)90089-5.

[33] B. G. Streetman and S. K. Banerjee, *Solid State Electronic Devices*. Upper Saddle River, NJ, USA: Prentice-Hall, 2006.

[34] A. Segal, O. Shaya, M. Karpovski, and A. Gerber, "Asymmetric field dependence of magnetoresistance in magnetic films," *Phys. Rev. B, Condens. Matter*, vol. 79, no. 14, Apr. 2009, Art. no. 144434, doi: 10.1103/PhysRevB.79.144434.

[35] P. G. N. De Vegvar, L. P. Lévy, and T. A. Fulton, "Conductance fluctuations of mesoscopic spin glasses," *Phys. Rev. Lett.*, vol. 66, no. 18, pp. 2380–2383, Jul. 2002, doi: 10.1103/physrevlett.66.2380.